

Article

The Effect of Hull Form Parameters on the Hydrodynamic Performance of a Bulk Carrier

Rui Deng ^{1,2}, Shigang Wang ^{1,2}, Yuxiao Hu ^{1,2}, Yuquan Wang ^{1,2} and Tiecheng Wu ^{1,2,*} 

¹ School of Marine Engineering and Technology, Sun Yat-sen University, Zhuhai 519000, China; dengr23@mail.sysu.edu.cn (R.D.); wangshg5@mail2.sysu.edu.cn (S.W.); huyx73@mail2.sysu.edu.cn (Y.H.); wangyq297@mail2.sysu.edu.cn (Y.W.)

² Southern Marine Science and Engineering Guangdong Laboratory (Zhuhai), Zhuhai 519000, China

* Correspondence: wutch7@mail.sysu.edu.cn; Tel.: +86-187-4514-7797

Abstract: In this study, the effect of joint optimization of the principal dimensions and hull form on the hydrodynamic performance of a bulk carrier was studied. In the first part of the joint optimization process, fast principal-dimension optimization of the origin parent ship considering the integrated performance of ship resistance, seakeeping, and maneuverability, as well as their relationships with the principal dimensions were analyzed in detail based on the ship resistance, seakeeping qualities, and maneuverability empirical methods of Holtrop and Mennen, Bales, and K and T indices, respectively. A new parent ship was chosen from 496 sets of hulls after comprehensive consideration. In the remaining part, a further hull form optimization was performed on the new parent ship according to the minimum wave-making resistance. The obtained results demonstrate that: (a) For the case in which the principal dimension of the original parent-type ship is different from that of the owner's target ship, within the bounds of the relevant constraints from the owner, an excellent parent ship can be obtained by principal-dimension optimization; (b) the joint optimization method considering the principal dimension and hull form optimization can further explore the optimization space and provide a better hull.

Keywords: principal-dimension optimization; ship resistance; seakeeping; maneuverability; Holtrop and Mennen's empirical methods; towing tank test



Citation: Deng, R.; Wang, S.; Hu, Y.; Wang, Y.; Wu, T. The Effect of Hull Form Parameters on the Hydrodynamic Performance of a Bulk Carrier. *J. Mar. Sci. Eng.* **2021**, *9*, 373. <https://doi.org/10.3390/jmse9040373>

Academic Editor: Kostas A. Belibassakis

Received: 13 March 2021
Accepted: 30 March 2021
Published: 1 April 2021

Publisher's Note: MDPI stays neutral with regard to jurisdictional claims in published maps and institutional affiliations.



Copyright: © 2021 by the authors. Licensee MDPI, Basel, Switzerland. This article is an open access article distributed under the terms and conditions of the Creative Commons Attribution (CC BY) license (<https://creativecommons.org/licenses/by/4.0/>).

1. Introduction

To reduce maritime greenhouse gas (GHG) emissions to reach the International Maritime Organization (IMO) 2050 target, new energy-efficient ships are urgently needed. Although these energy-efficient designs have a higher newbuild cost, the savings on fuel consumption and, in turn, the cost, tend to be considerably larger than the additional newbuild cost [1–4].

Among the various aspects of ship performance, hull form optimization has long focused on minimizing ship resistance. For certain hull forms, hull form optimization can reduce resistance. Sariöz [5] presented an optimization approach to be used in the preliminary design stage to create a high-quality ship hull form geometry. Hong et al. [6] developed a self-blending method to modify and optimize a bulbous bow. The shape of the bulbous bow of a fishing vessel was optimized, and the resistance was reduced by 2%. Rotteveel et al. [7] analyzed the optimization of propulsion power for various water depths using a parametric inland ship stern shape. Cerka et al. [8] presented a numerical simulation of hull form optimization of a multi-purpose catamaran-type research vessel based on the method of successive approximations. Deng et al. [9] used nonlinear programming and genetic algorithms to optimize the hull form and achieved promising results. Cheng et al. [10] used a new hull surface automatic modification method based on Delaunay triangulation to perform hull form optimization, which can significantly improve the optimization efficiency. Hou [11] presented the hull form optimization design

method for minimum Energy Efficiency Operation Index (EEOI), and four case studies were conducted to verify the feasibility and superiority of the novel approach. Zheng et al. [12] took numerical functions and the surface combatant model DTMB 5415 as the research objectives for knowledge extraction by combining the partial correlation analysis and self-organizing map (SOM) based on optimization data. Kim et al. [13] studied an efficient and effective hull surface modification technique for the Computational Fluid Dynamics (CFD)-based hull form optimization. Numerical results obtained in this study have shown that the present hull surface modification technique can produce smooth hull forms with reduced drag effectively and efficiently in the CFD-based hull form optimization. Feng et al. [14] performed an experimental and numerical study of multidisciplinary design optimization to improve the resistance performance and wake field quality of a vessel. Lin et al. [15] set up an automatic design optimization of a small waterplane area twin-hull (SWATH) that provides accurate flow prediction and is integrated into the optimization module. They obtained lower resistance than the original hull, which shows the effectiveness of the optimization. Seok et al. [16] applied the design of experiments and CFD to improve the bow shape of a tanker hull. The results show that the added resistance of the improved hull form is reduced by 52%. Priftis et al. [17] applied a holistic optimization design approach to study the parametric design and multi-objective optimization of ships under uncertainty. Papanikolaou et al. [18] performed a numerical and experimental optimization study on a fast, zero-emission catamaran. Jeong et al. [19] proposed two methods for comparing the mesh deformation method for hull form optimization. Various bow shapes of the Japan Bulk Carrier were applied to validate the applicability of the methods. The proposed mesh deformation method was efficient and effective for CFD-based hull form optimization.

However, in general, hull form optimization does not result in significant changes to the original hull form, and the corresponding effect on the resistance reduction becomes increasingly limited with the improvement in the hull form. Compared with hull form optimization, the principal dimensions of the hull can have a more significant impact on the hydrodynamic performance of the ship; however, they are usually determined by the usage requirements, parent ship dimensions, and other constraints in the initial stage of ship design, following which the modification of the principal dimensions is seldom considered. Therefore, few researchers have conducted studies on resistance reduction based on principal-dimension optimization. Zhang et al. [20] used regression analysis to study the sensitivity of the resistance to the principal dimension of the hull form; the principal dimension parameters with the most significant effects on the total resistance were identified, and the ship resistance was significantly reduced by changing the principal dimensions. Pechenyuk [21] proposed a wave-based optimization method for hull form design, which changes the displacement volume distribution by varying the principal dimensions and thus optimizes the transverse and scattered waves induced. The optimized design of the hull provided the best displacement volume distribution, and the resistance was reduced by 8.9% compared with that of the parent ship. Lindstad et al. [1,4,22–24] studied how hull forms can be made more energy efficient for realistic sea conditions by modifying the main ratios among beam, draught, and length to reduce the block coefficients while keeping the cargo-carrying capacity unchanged. In addition to resistance optimization, Ouahsine et al. [25,26] proposed a numerical method based on the combination of a mathematical model of nonlinear transient ship maneuvering motion in the horizontal plane and mathematical programming techniques; this method was validated by the turning circle and zigzag maneuvers based on experimental data of sea trials of the 190,000 dwt oil tanker. Subsequently, they developed a numerical model to predict ship maneuvering in a confined waterway using a nonlinear model with optimization techniques to identify the hydrodynamic coefficients accurately.

Some studies have been performed for hull form and principal-dimension optimization of ships. Few scholars have conducted relevant research on the joint optimization of principal dimensions and hull form of ships considering the integrated performance of ship resistance, seakeeping, and maneuverability. Thus, there are still some important

aspects that need to be investigated further regarding this topic, such as the accuracy and applicability of empirical methods for the rapid prediction of ship resistance, seakeeping, and maneuverability; accuracy correction of empirical methods for given ship types; and relationships of resistance, seakeeping, and maneuverability performance with the principal dimensions.

In this study, the effect of joint optimization of the principal dimensions and hull form on the hydrodynamic performance of a bulk carrier (origin parent ship) is studied based on empirical methods and towing tank tests, considering the integrated performance of ship resistance, seakeeping, and maneuverability. First, empirical methods of ship resistance, seakeeping, and maneuverability are introduced, and then the accuracy correction of the resistance empirical method based on CFD for the given ship is studied. Second, the resistance, seakeeping, and maneuverability of 496 sets of hulls with different principal dimensions are calculated using the modified empirical methods, and the relationships of resistance, seakeeping, and maneuverability of the hull with the principal dimensions are analyzed in detail. Thereafter, a new parent ship with $L = 136.0$ m and $B = 18.38$ m is chosen through the systematic analysis of principal-dimension optimization. Finally, further hull form optimization and verification based on the new parent ship by the towing tank test are presented. The remainder of this paper is organized as follows. Section 1 discusses the literature review of the form and principal-dimension optimization of ships. The geometric model and offset point information of the parent ship are described in Section 2. In Section 3, the ship resistance, seakeeping qualities, and maneuverability empirical methods of Holtrop and Mennen, Bales, and K and T indices are described, respectively. The accuracy correction of Holtrop and Mennen's empirical method based on CFD for the given ship type is studied in detail. Section 4 presents the relationships between resistance, seakeeping, and maneuverability performance with the principal dimensions. Section 5 describes the optimization procedure. Further hull foam optimization and verification based on the selected new parent ship are discussed in Section 6. Section 7 provides a summary of this study.

2. Geometric Model and Information of the Parent Ship

In this study, a bulk carrier was treated as the origin parent ship, with a length of 132 m, width of 18.2 m, and draft of 5.9 m, block coefficient of 0.6025, displacement of 8806.6 t, and designed speed of 19 kn. The 3-dimensional geometric model and the offset points used for calculation are shown in Figure 1.

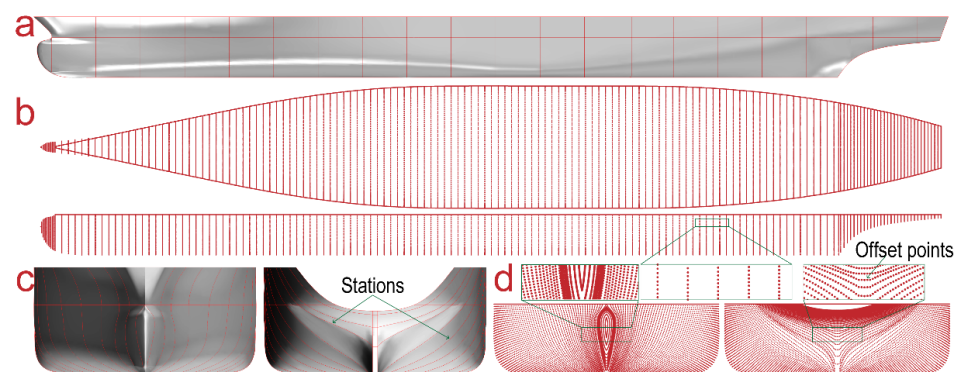


Figure 1. Geometric model and offset points of the parent ship: (a) Side view of the geometric model of the parent ship; (b) top and side views of the offset points of the parent ship; (c) front and stern views of the geometric model of the parent ship; (d) front and stern views of the offset points of the parent ship.

The required offsets were extracted and calculated by the software GAMBIT which is a registered trademark of Fluent, Inc (now owned by ANSYS Inc, Canonsburg, PA, USA) (Figure 1). The stations were set every 0.2 m for the bow, every 1.0 m for the hull, and every

0.5 m for the stern, such that the underwater part of the hull was divided into 161 stations from the bow apex to the stern. A total of 70 offset points were obtained for each station line, and the maximum distance between the offset points was approximately 0.14 m. A total of 13,651 offset points were obtained from the waterline, and the maximum distance between the offset points was approximately 0.44 m. This yielded a total of 24,921 offset points to ensure that the hull geometric information was accurately captured.

3. Methodology

Owing to the large Reynolds numbers of full-scale ships, the numerical calculation of their viscous wake fields based on the CFD method requires many cells and specific turbulence models, 2-phase flow models, and degree of freedom motion models, leading to a high threshold of numerical skills and long computation time. Therefore, this method is not applicable for the comparison of multiple schemes in the preliminary design stage. In contrast, existing empirical methods based on regression analysis of model tests and trial data of many ships have good usability and are less time-consuming. Although the calculation accuracy for a particular hull form is limited, it can accurately reflect the changes in the hydrodynamic performance of the ship as the principal dimension changes. Therefore, in this study, the empirical methods of Holtrop and Mennen, Bales, and *K* and *T* exponents were used in principal-dimension optimization to calculate the resistance, seakeeping, and maneuverability of a series of hull forms.

3.1. Holtrop and Mennen’s Empirical Methods of Ship Resistance

At present, there are many empirical formula methods for resistance, such as Ayre’s method, Lap–Keller’s method, and Holtrop and Mennen’s method. Ayre and Lap–Keller’s methods are based on the statistical data of ship types of the 1940s and 1950s. Thus, obvious errors arise from new types of ships in the estimation after the late 1980s. In the early 1980s, Holtrop and Mennen developed a resistance prediction method based on regression analysis of model tests and trial data of Marine Research Institute Netherlands (MARIN), the model basin in Wageningen, The Netherlands [27–31]. Holtrop and Mennen’s method was arguably the most popular method for estimating the resistance and horsepower of displacement-type ships. It was based on the regression analysis of a vast range of model tests and trial data, which provided wide applicability [32]. Holtrop and Mennen’s method defines the total resistance as:

$$R_T = R_F + R_P + R_W, \tag{1}$$

where R_T is the total resistance, and R_F , R_P , and R_W represent the frictional, pressure, and wave resistances, respectively. The friction resistance is corrected by introducing the form factor k , which affects the estimation of the residuary resistance, and the pressure resistance is included in the friction resistance. The frictional resistance R_F is computed on the basis of the international towing tank conference (ITTC) 1957 model–ship correlation line coefficient C_F as the resistance of a flat plate with wetted surface S :

$$R_F(1 + k) = R_F + R_P, \tag{2}$$

$$R_F = 1/2C_F\rho V^2S, C_F = 0.075/(\log \text{Re} - 2)^2, \tag{3}$$

To estimate the wave resistance R_W , Holtrop defines R_W as the range of Froude numbers into 3 sections:

$$R_W = \begin{cases} c_1c_2c_5\rho g \nabla \cdot e^{m_1Fr^d+m_4 \cos(\lambda Fr^{-2})} & \text{if } Fr \leq 0.4 \\ R_W(0.4) + \frac{(20Fr-8)}{3}[R_W(0.55) - R_W(0.4)] & \text{if } 0.4 < Fr \leq 0.55 \\ c_{17}c_2c_5\rho g \nabla \cdot e^{m_3Fr^d+m_4 \cos(\lambda Fr^{-2})} & \text{if } Fr > 0.55 \end{cases} . \tag{4}$$

In Equations (2)–(4), ρ is the density of sea (fresh) water, V is the velocity of the ship, ∇ is the volumetric displacement, and Re and Fr are the Reynolds and Froude numbers,

respectively. Furthermore, $c_1, c_2, c_5, c_{17}, d, \lambda, m_1, m_3,$ and m_4 are coefficients for the wave resistance computation in Equation (4), and the detailed description, definition, and calculation equations of the above coefficients can be found in references [27–32].

For the empirical formula methods proposed in the ship resistance evaluation method section, the methods should be first compared to determine the one to be applied. The resistance of 3 types of ships [33] (25,000 t tanker, 82,000 t bulk carrier, and 900 TEU container ship) was predicted by the empirical formula methods and compared with the experimental data, as shown in Figure 2.

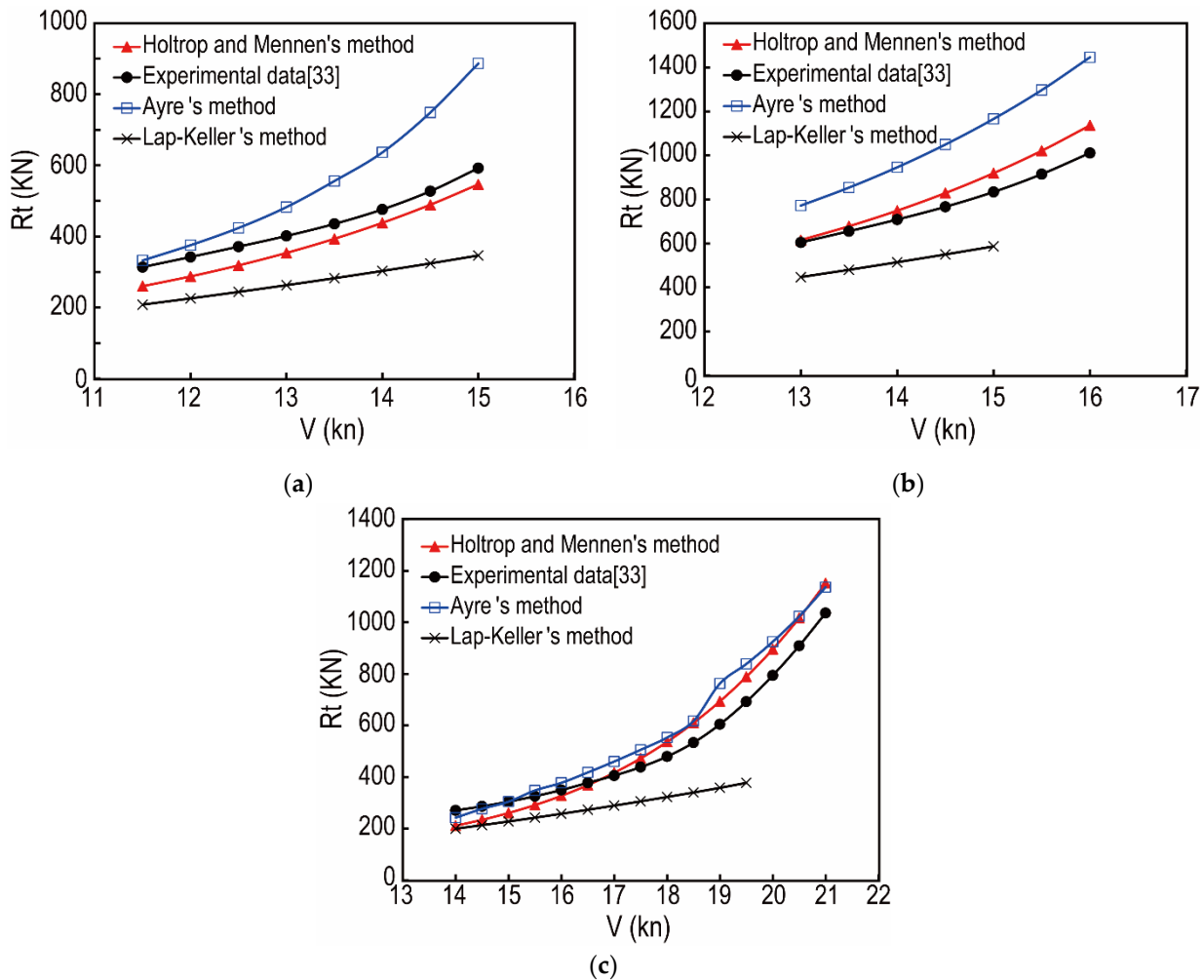


Figure 2. Comparison between the results of the Ayre’s, Lap–Keller’s, Holtrop and Mennen’s methods and experimental data. (a) 25,000 t tanker; (b) 82,000 t bulk carrier; (c) 900 TEU container ship.

From the comparison of the results in Figure 2, it can be observed that the calculation results of various empirical formula methods can basically maintain the tendency as the experimental results and can reflect the resistance characteristics of the ship. Owing to the different applicability of each method, the errors for different ship types are also different; Ayre and Lap–Keller’s methods have better accuracy at low speeds and gradually become misaligned as the speed increases. These methods are based on the statistical data of ship types in the 1940s and the 1950s, and the resistance estimation errors for emerging ship types are relatively large. Although the Holtrop and Mennen’s method has certain errors, it is generally better than the other two methods. In chronological order, this method was also the latest resistance empirical formula method, which has certain credibility for the estimation of modern ship types. Therefore, in terms of resistance prediction, the

Holtrop and Mennen’s method can be recommended as a credible method for estimating the resistance of the target ship.

3.2. Brief Description of Bales’s Empirical Method for Ship Seakeeping Performance

Bales calculated the seakeeping properties of 20 destroyers, used 6 geometric characteristics C_{WF} , C_{WA} , T_d/L , C/L , C_{VPF} , and C_{VPA} as variables for regression analysis, and established the relationship between the seakeeping rank factor R and geometric characteristics. The seakeeping prediction model proposed by N.K. Bales [34,35] was adopted by the ship design department of the US Navy and was later promoted and can be used in a variety of ship types. The rank factor R is defined as follows:

$$\hat{R} = 8.422 + 45.104C_{WF} + 10.078C_{WA} - 378.465\frac{T_d}{L} + 1.273\frac{C}{L} - 23.501C_{VPF} - 15.875C_{VPA} \quad (5)$$

where \hat{R} is the estimated value of R ; C is the distance from Station 0 to the cut-up point; T_d and L are the draft and length between the perpendiculars of the ship; C_{WF} and C_{WA} represent the water-plane coefficients forward and aft of amidships, respectively; and C_{VPF} and C_{VPA} are the vertical prismatic coefficients forward and aft of amidships, respectively. The rank factor R indicates the degree of seakeeping performance: A larger value indicates better performance. The detailed description, definition, and calculation equations of the above coefficients can be found in references [34,35].

3.3. Brief Description of K and T Indices Empirical Methods for Ship Maneuverability

Nomoto [36,37] studied the problem of ship maneuverability from the viewpoint of control engineering based on the linear equation of ship maneuverability motion and regarded the various maneuvering motions caused by changing the rudder angle as the response of the output maneuvering motion to the input rudder angle. In addition, a second-order maneuvering motion equation was derived, which was also called K . Nomoto’s model. The exponents K and T of K . Nomoto’s model can define the maneuverability of the ship, which has a clear physical meaning. The K index reflects the turning ability of the ship and is called the turning ability index; the T index represents the ship’s rapid response to the rudder and navigation stability and is called the turning lag index. K and T are collectively referred to as the ship’s maneuverability index. Ships with good maneuverability should have a large positive K value and a small positive T value. Zhang et al. [38,39], based on the research of Hong [40] and Yao [41] by increasing the number and types of statistical ships, and considering the influence of nonlinear factors between the data volumes, used the parameters of 59 ships as samples, established the quaternion second-order polynomial regression mathematical model, and obtained a statistical regression formula. The results of this formula were compared with the Z-shaped experimental results of the ship, which were not in the statistical samples, to verify the validity of the equation. The estimation formulae for K and T are defined as follows:

$$\hat{K} = 47.875 - 2.64\frac{L}{B} + 0.004\frac{LT_d}{A_R} + 66.589C_b^2 - 112.702C_b + 3.826C_b\frac{L}{B} - 0.393C_b\frac{B}{T_d}, \quad (6)$$

$$\hat{T} = 26.464 + 0.408C_b\frac{LT_d}{A_R} - 0.033\frac{L}{B}\frac{LT_d}{A_R} - 79.114C_b + 0.757\frac{L}{B} + 46.129C_b^2. \quad (7)$$

where \hat{K} and \hat{T} are the estimated values of K and T , respectively; T_d , B , and L are the draft, breadth, and length between the perpendiculars of the ship, and C_b and A_R represent the block coefficient and rudder area, respectively. The maneuverability index P is defined as $P = K/T$, in which a larger P -value indicates better ship maneuverability.

3.4. Accuracy Correction of Holtrop and Mennen's Empirical Method Based on CFD for the Given Ship Type

In the principal-dimension optimization part, the resistance performance was the most important aspect of the hydrodynamic performance, followed by seakeeping and maneuverability. Accuracy correction was only performed for the empirical method of resistance. Because the ship used in the establishment of Holtrop and Mennen's empirical method was somewhat different from the one used in this study, and as described in Section 3.1, directly using this method to calculate the resistance of a ship will result in certain potential errors. Therefore, it was necessary to improve the accuracy of Holtrop and Mennen's empirical method according to the ship used in this study. In the process of correction for the empirical method of resistance, the toolbox commercial CFD software STAR CCM+ was used to calculate the total resistance of the parent ship at speeds of 9, 11, 13, 15, 17, 19, 21, and 23 kn, and the detailed experience and description of the numerical calculation strategy can be found in our previous research [42,43]. The total resistance was composed of friction and residual resistances. Because the frictional resistance in the Holtrop and Mennen's method was calculated using the ITTC-1957 formula, it can be assumed that the frictional resistance was correct after considerable experience, and the error of the method only comes from the residual resistance. Subsequently, the residual resistance was separated from the numerical results, and the residual resistance calculated by Holtrop was compared. The ratio of the two parts was used to establish a correction coefficient related to the Fr number, and then the residual resistance term of Holtrop and Mennen's empirical method was corrected. Finally, principal-dimension optimization was performed based on the modified method with acceptable accuracy.

A comparison between the prediction results of the original and modified Holtrop and Mennen's method and the CFD results of the full-scale ship is presented in Figure 3.

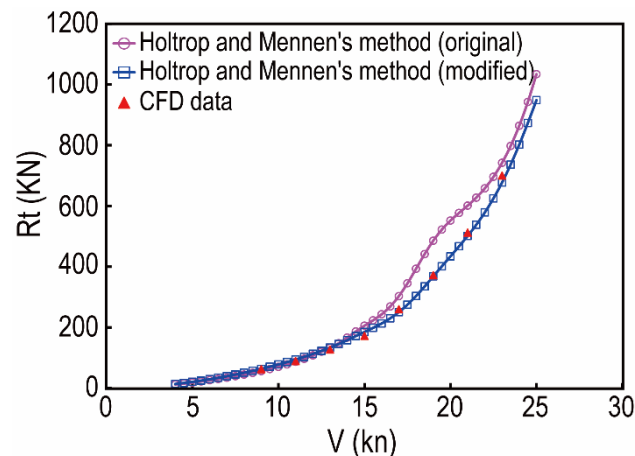


Figure 3. Comparison between the results of the original and modified Holtrop and Mennen's method and the CFD data.

As indicated by Figure 3, the modified Holtrop and Mennen's method demonstrates good agreement with the CFD results, better pertinence, and accuracy. Thus, it can be adopted as a reliable approach for subsequent research. Although the correction coefficient for Holtrop and Mennen's empirical formula in this study is only suitable for the parent ship and is not applicable to all the ships, the correction strategy employed can be implemented for specific ship types and has universal applicability.

4. Relationships of Resistance, Seakeeping, and Maneuverability Performance with the Principal Dimensions

The variation of the principal dimensions in the study was constrained to within $\pm 15\%$ and $+15\%$ of the original ship length, beam: The length varied between $112.2 \text{ m} \leq L \leq 151.8 \text{ m}$, with one length selected every 1% of the baseline length (132 m), for a total of 31 lengths;

the ship beam varied within the range of $18.20 \text{ m} \leq B \leq 20.93 \text{ m}$, with one ship beam selected every 1% of the baseline ship beam (18.20 m), for a total of 15 ship beams. The ship's length and beam were considered as the main variables, and the draft was considered as a secondary variable. The draft was determined after selecting different ship lengths and beams, while keeping the displacement constant at 8600 t, yielding a total of 496 sets of hulls with different principal dimensions. Among them, the change in principal dimensions met the regulations and owner requirements, and the general arrangement of the ship. The relationships of the total hull resistance, seakeeping, and maneuverability with the length and beam at the design speed (19 kn) are shown in Figure 4.

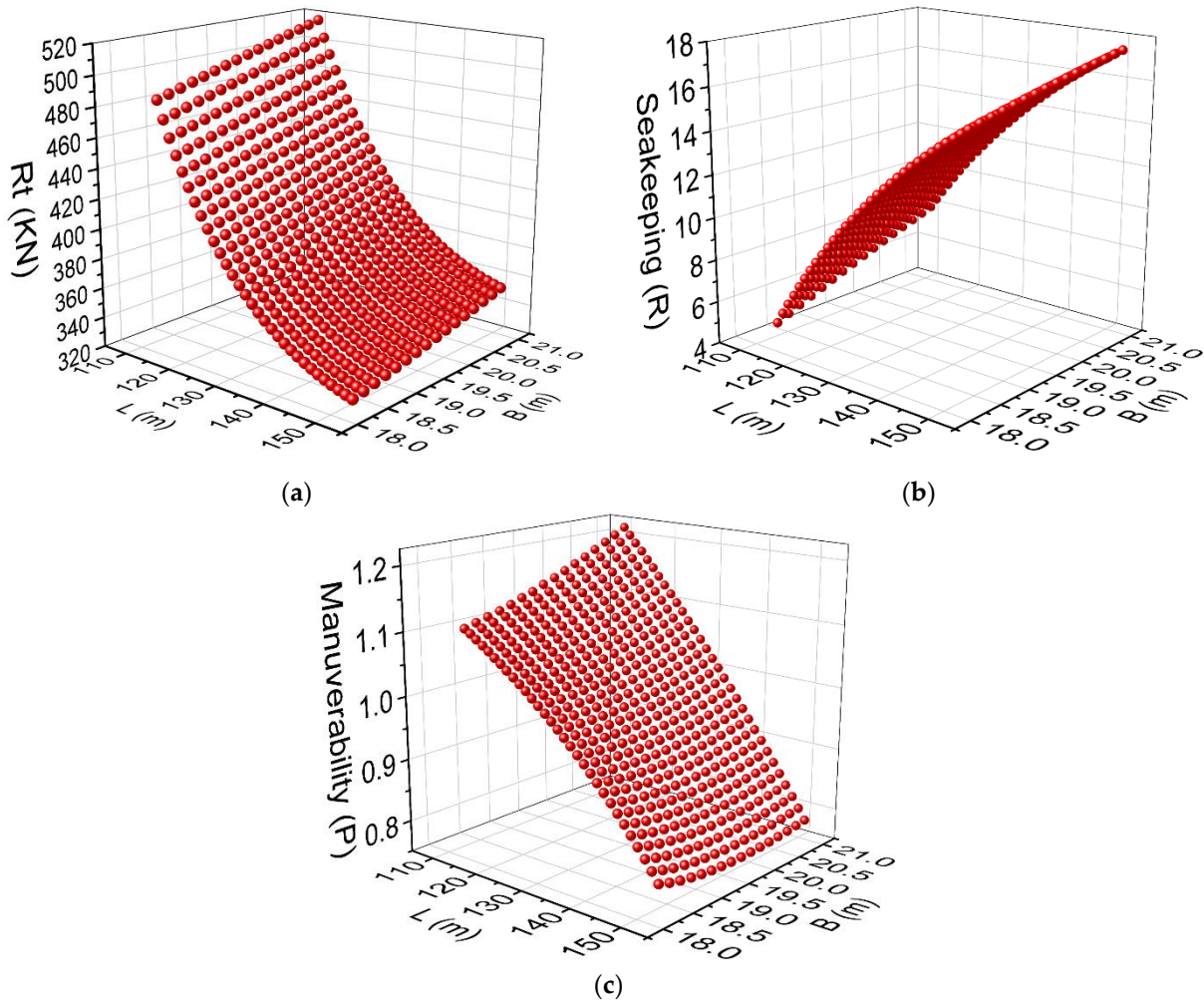


Figure 4. Relationships of various hydrodynamic performances with the principal dimensions: (a) ship resistance; (b) rank factor R of seakeeping performance; (c) maneuverability index $P (P = K/T)$.

As shown in Figure 4, while the displacement was kept constant, the resistance monotonically increased with the hull beam and monotonically decreased with increasing ship length. The seakeeping index rapidly increased with ship length and slightly increased with increasing hull beam, which may be resulted from a decrease in the draft. The maneuverability index exhibited opposite change tendencies: as the ship length increased, the maneuverability index first increased and then decreased, whereas as the ship beam increased, the maneuverability index first decreased and then increased.

5. Optimization Procedure

5.1. Rough Selection from Large Amounts of Data

A rough selection from large amounts of data set of performance is discussed in this subsection. The schematic diagram of the optimization process is shown in Figure 5. First of all, we established 496 sets of hulls with different principal dimensions based on the original parent ship, with the variation interval of the principal dimension as the constraint condition. The variation interval of the principal dimension was described in detail in Section 4. Secondly, the hull resistance, seakeeping, and maneuverability indices were calculated for 496 selected sets of principal dimensions using resistance, seakeeping qualities, and maneuverability empirical methods of Holtrop and Mennen, Bales, and K and T indices, respectively. In addition, we got a data set of ship performance. Thirdly, a rough selection from large amounts of data was carried out based on constraints and selection conditions. The constraints and selection conditions were as follows: (a) The resistance of the hulls should be smaller than that of the parent ship at the design speed (19 kn); (b) the change ranges of seakeeping and maneuverability are within 21% and 9%, respectively. Finally, we got five sets of hulls through the rough selection.

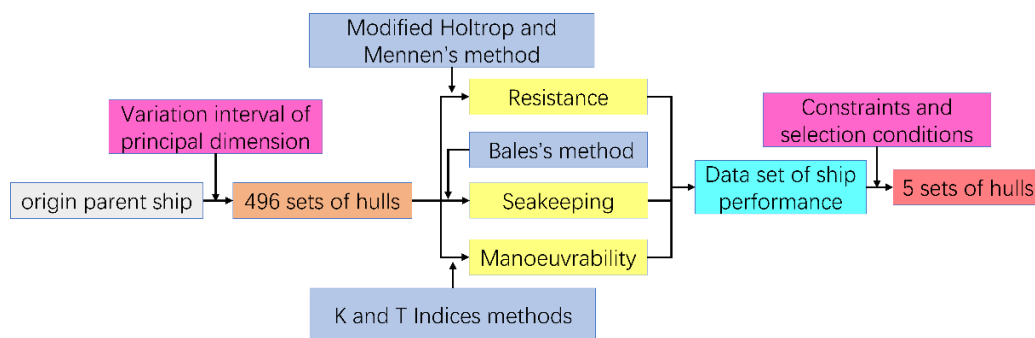


Figure 5. Schematic diagram of rough selection from large amounts of data in the optimization process.

The performance parameters for the five sets of principal dimensions and the parent ship at a speed of 19 kn are presented in Table 1.

Table 1. Performance parameters for the different principal dimensions and parent ship at 19 kn.

NO.	L (m)	B (m)	T (m)	C _B	C _P	C _{WP}	S (m ²)	RT (KN)	Seakeeping (R)	Maneuverability (P)
1	141.2	18.38	5.555	0.6027	0.6158	0.7089	2838	345.1	13.90	0.9051
2	139.9	18.38	5.608	0.6025	0.6514	0.7114	2822	347.9	13.62	0.9173
3	138.6	18.38	5.661	0.6025	0.6507	0.7596	2806	350.9	13.32	0.9291
4	137.3	18.38	5.715	0.6025	0.6502	0.7161	2790	354.2	13.03	0.9406
5	136.0	18.38	5.771	0.6023	0.6496	0.7814	2774	357.7	12.72	0.9518
Original parent ship	132.0	18.20	6.003	0.6025	0.6256	0.7724	2723	368.1	11.57	0.9851

As indicated in Table 1, the hulls of the five selected principal-dimension combinations had a lower resistance in the 16–20 kn speed range and also larger seakeeping and maneuverability indices. This indicates that the vessels of these five principal-dimension combinations had better seakeeping and maneuverability.

5.2. Effect Analysis of Principal-Dimension for the Selected Five Sets of Hulls

To analyze the effects of principal-dimension optimization on the resistance, seakeeping, and maneuverability, the resistance of the five hull forms and the parent ship within the speed range of 4–25 kn were analyzed, and the results are shown in Figure 6.

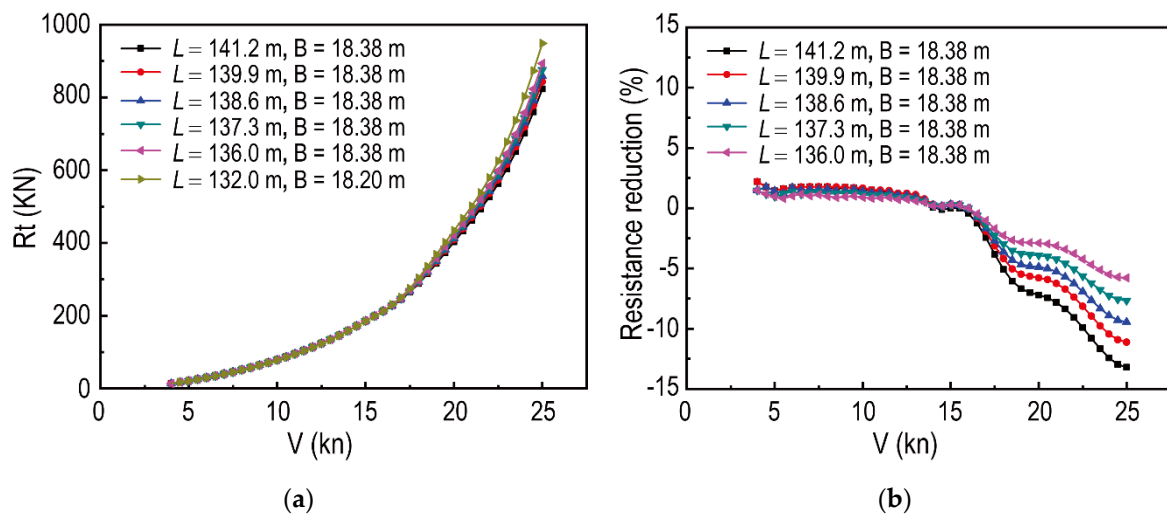


Figure 6. Comparison of the total resistance and resistance reduction rates before and after principal-dimension optimization: (a) total resistance; (b) resistance reduction rates.

As shown in Figure 6, when the speed was lower than 17.5 kn, the effect of principal-dimension optimization was insignificant, and the resistance of the optimized hull form was not significantly lower than that of the parent ship. When the speed was higher than 17.5 kn, the effect of the principal-dimension optimization was more significant, and the resistance of the hull forms after the principal dimensions were changed was significantly lower than that of the parent ship. Furthermore, the resistance is decreased when the ship length is increased, mainly because wave-making resistance can be reduced by increasing the ship length at high speed. Additionally, the ship beams were identical for the five hull forms, with good resistance performance. This implies that for the hull form adopted in this study, if the displacement remains adopted and the principal dimensions are altered to reduce the resistance at high speed, an optimal value can be obtained for the ship beam. In addition, it is helpful to increase the ship length and reduce the draft for resistance reduction at high speed. For the selection of one hull form from the five sets of principal-dimension combinations, if the key consideration is the resistance at the design speed (19 kn), the principal dimensions of the hull form with the minimum resistance are $L = 141.24$ m and $B = 18.38$ m, indicating a 6.7% reduction in resistance, 18.4% improvement in seakeeping, and 8% reduction in maneuverability compared with the parent ship.

Based on the comparison of the resistance performance before and after the principal-dimension optimization, the seakeeping and maneuverability of the five selected hull forms within the range of 16–20 kn were further compared, and the results are shown in Figure 7. When the ship beam was fixed, the seakeeping gradually increased with the increasing ship length, and the seakeeping index was maximized when ship length was $L = 141.2$ m, indicating that increasing the ship length and reducing the draft can improve the seakeeping under the same displacement (see Figure 7a). As shown in Figure 7b, the maneuverability exhibited the opposite tendency when increasing ship length within the speed range of interest. When the speed was less than 17 kn, the maneuverability index was increased with the ship length, indicating better maneuverability; when the speed was higher than 17 kn, the maneuverability index was decreased with ship length. Hence, the maneuverability did not vary monotonically with ship length over a wider speed range, and increasing the ship length at high speed did not benefit the maneuverability of the examined hull form. The variation of the maneuverability with respect to the ship beam was more significant when the ship beam was smaller than 17 m. For the hull with $L = 141.2$ m and $B = 18.38$ m, the maneuverability was good at a low speed but poor at high speed. The hull with $L = 136.0$ m and $B = 18.38$ m yielded the best maneuverability at high speed, and the maneuverability was improved by 5.16% when the speed was 19 kn compared with the case of the hull with $L = 141.2$ m and $B = 18.38$ m.

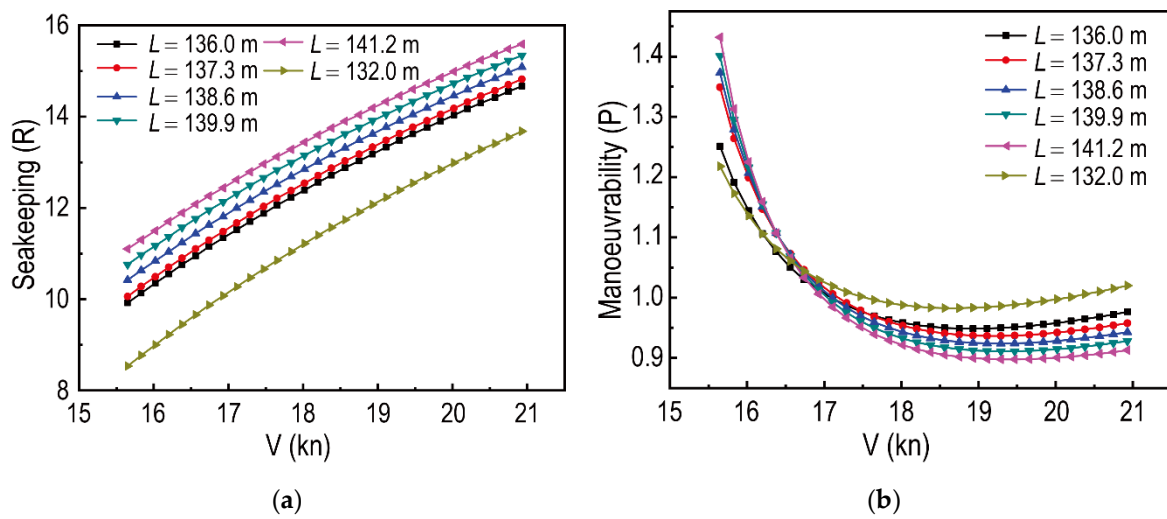


Figure 7. Variation of seakeeping and maneuverability with the principal dimensions: (a) Seakeeping; (b) maneuverability.

5.3. Further Selection from the Five Sets of Principal-Dimension Combinations

A further selection from the five sets of principal-dimension combinations is discussed in this subsection. According to the law of actual ship manufacturing cost, the increase of ship length under the same conditions will directly lead to the increase in shipbuilding cost. In the further selection process, in addition to considering the ship’s resistance, seakeeping, and maneuverability performance, it also comprehensively considers the additional construction costs caused by the increase in the length of the ship.

By comprehensively considering the ship’s length, resistance, seakeeping, and maneuverability, we have established a comprehensive optimization index, and the comprehensive optimization index Z is defined as follows:

$$Z = -2.5 \frac{L_i - L_0}{L_0} + \frac{|Rt_i - Rt_0|}{Rt_0} + 0.8 \frac{R_i - R_0}{R_0} + 0.8 \frac{P_i - P_0}{P_0} \tag{8}$$

Note: Compared with the parent ship, the five ship types have negative effects on the relative comprehensive optimization indexes of ship length and maneuverability, and “-” should be added, and the weights of length, resistance seakeeping, and maneuverability are 2.5, 1, 0.8, and 0.8, respectively.

Where L_i , Rt_i , R_i , and P_i are the length, resistance, rank factor of seakeeping performance and maneuverability index of the selected five sets of hulls, and L_0 , Rt_0 , R_0 , and P_0 are the length, resistance, rank factor of seakeeping performances and maneuverability index of the parent ship, respectively. The calculation results of the comprehensive index of the selected five sets of hulls are shown in Table 2.

Table 2. Comprehensive optimization calculation results of the selected five sets of hulls.

NO.	L (m)	B (m)	$\frac{L_i - L_0}{L_0}$	$\frac{ Rt_i - Rt_0 }{Rt_0}$	$\frac{R_i - R_0}{R_0}$	$\frac{P_i - P_0}{P_0}$	Z
1	141.2	18.38	0.0697	0.0625	0.2014	-0.0812	-0.01559
2	139.9	18.38	0.0598	0.0549	0.1772	-0.0688	-0.00788
3	138.6	18.38	0.0500	0.0467	0.1513	-0.0568	-0.0027
4	137.3	18.38	0.0402	0.0378	0.1263	-0.0452	0.00218
5	136.0	18.38	0.0303	0.0283	0.0994	-0.0338	0.00503

According to the comparative analysis of the five optimized hull forms, the hull form with L = 141.2 m and B = 183.38 m exhibited a good ship resistance but also a loss of maneuverability due to the increase in the ship length, which increased the production costs. By comprehensively considering the foregoing factors, it was found that while the

displacement was kept constant and only the principal dimensions were changed, five hull forms outperformed the parent ship with regard to the resistance performance, seakeeping, and maneuverability. The ship beam of these five hull forms was 18.38 m, which was higher than that of the parent ship. This is acceptable because an increase in the beam is helpful for improving stability. Both the resistance performance and seakeeping were improved with an increase in the length, but the maneuverability exhibited an initial improvement, followed by deterioration with increasing length. In this study, only the displacement was kept constant. However, in practice, an excessive ship length increased the lightship weight and reduced its effective loading capacity. Furthermore, a long and slender hull requires further strengthening of the hull structure. Therefore, although the main objective of this study was to improve the resistance performance, it was also necessary to consider the improvement of other aspects of the performance and the practical value of the optimized hull form. According to the calculation results in Table 2, it can be seen that the No.5 ship hull has the largest comprehensive optimization index Z. Therefore, after comprehensive consideration, the optimized hull form (new parent ship) with $L = 136.0$ m and $B = 18.38$ m was chosen.

6. Further Hull Form Optimization and Verification Based on the Selected New Parent Ship

After the principal dimensions were optimized, further hull form optimization was performed on the new parent ship ($L = 136.0$ m and $B = 18.38$ m) according to the minimum wave-making resistance. Several previous studies reported results in this area, and thus will not be described here. After hull form optimization, no significant changes were made to the hull form. The optimized hull form was compared with the new parent ship, as shown in Figure 8, in which the red dashed line indicates the body plan lines of the optimized hull form, and the solid black line indicates the body plan line of the new parent ship. On this basis, the ship model of the new parent ship and the optimized hull form were created at a scale ratio of $\lambda = 22$, and a towing tank test was performed. The main parameters of the optimized hull ship in the model and the full scale are presented in Table 3.

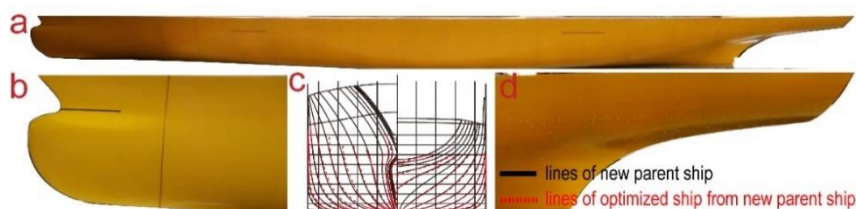


Figure 8. Ship model for towing tank experiment: (a) side view of the ship model of the optimized hull from new parent ship; (b) sketch of the bow; (c) front and stern views of the ship plan line of hulls; (d) sketch of the stern.

Table 3. Main parameters of the optimized hull from the new parent ship.

Parameters	Symbols	Model Scale	Ship Scale
Length overall (m)	Loa	6.5818	147.80
Length on waterline (m)	Lwl	6.1791	136.00
Beam (m)	B	0.8354	18.38
Depth (m)	D	0.4095	9.00

Figure 9 shows the resistance of the hull before and after optimization, including the experimental data, empirical formula data, and resistance reduction. The red line is the experimental data of the new parent ship, the green line is the experimental data of the optimized hull of the new parent ship, and the purple diamond points are the Holtrop and Mennen’s empirical formula (modified) data. Because the new parent ship was formed

by the principal-dimension optimization of the original parent ship, the new parent ship had undergone a round of resistance optimization. Under the condition that the hull form type did not change significantly, the maximum resistance reduction of the hull optimized from the new parent ship was 1.5%. In addition, a comparison between the experimental data and Holtrop and Mennen’s empirical formula (modified) data of the new parent ship shows that the accuracy correction of the empirical method based on CFD for the given ship type is reliable.

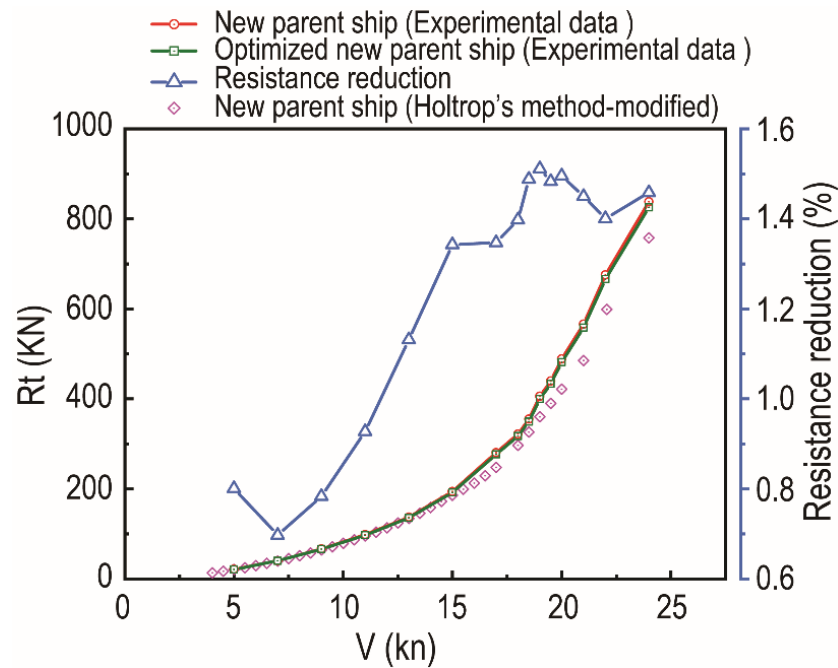


Figure 9. Resistance of the hull before and after optimization, including experimental data, empirical formula data, and resistance reduction.

Figure 10 shows the waveform of the hull in the towing tank before and after optimization, including the bow wave, shoulder wave, and wave scars. From the waveform information of the same viewing angle in Figure 9, it can be seen that the optimized ship has a smaller wave-making range. Because the length of the waterline remains unchanged before and after the optimization, the frictional resistance (1957 ITTC empirical formula) of the ship remains unchanged, and the reduction in the resistance of the ship is mainly reflected in the residual resistance component, including the wave-making resistance. The above waveform information also provides this evidence.

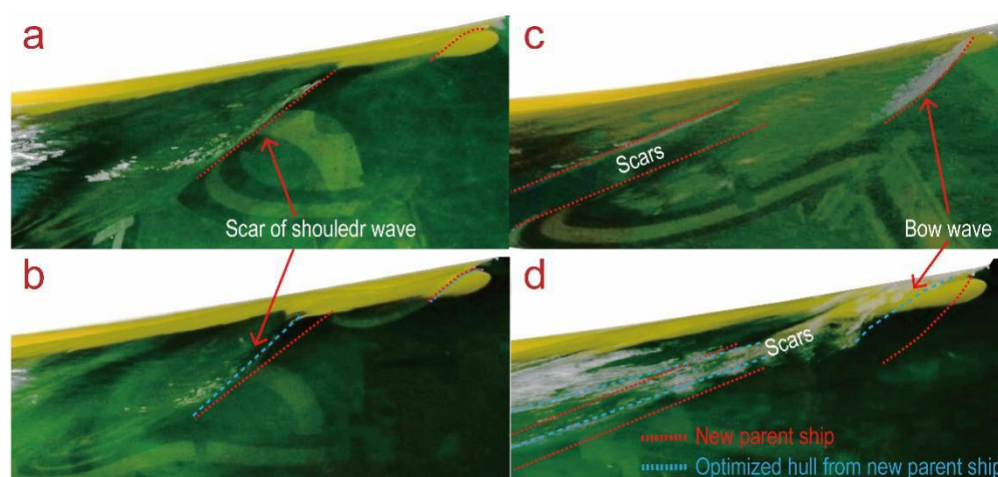


Figure 10. Wave form of the ships under different speeds: (a) Wave form of the new parent ship at the speed of 13 kn; (b) wave form of the optimized hull from new parent ship at the speed of 13 kn; (c) wave form of the new parent ship at the speed of 19 kn; (d) wave form of the optimized hull from new parent ship at the speed of 19 kn.

7. Conclusions

Joint optimization of the principal dimensions and hull form on the hydrodynamic performance of a bulk carrier (origin parent ship) considering the integrated performance of ship resistance, seakeeping, and maneuverability was studied based on empirical methods and towing tank tests. The following conclusions were drawn:

1. Holtrop and Mennen's method is arguably the most popular method for estimating the resistance of displacement-type ships. The results obtained by the modified Holtrop method based on CFD for the given ship in the present study exhibited good agreement with the CFD and experimental data of the towing tank, good pertinence accuracy.
2. Variations of the principal dimensions affected ship resistance, seakeeping, and maneuverability. Within the requirements of regulations, owner's requirements, and general arrangement of the ship, principal-dimension optimization can improve the performance of the original parent ship and provide a new parent ship for further hull form optimization.
3. The joint optimization method considering the principal dimension and hull form optimization can further explore the optimization space and provide a better hull.

Some research limitations in this paper: All the optimization in this paper were performed conditions of calm water, without considering the influence of wind and waves; Optimization targets only focus on resistance, seakeeping, and maneuverability. There is no verification and attempt to adopt more updated empirical formula methods.

Author Contributions: Conceptualization, R.D. and T.W.; methodology, R.D.; software, R.D.; validation, Y.H. and Y.W.; formal analysis, R.D.; investigation, R.D.; resources, T.W.; data curation, T.W.; writing—original draft preparation, S.W., R.D. and T.W.; writing—review and editing, R.D. and T.W.; visualization, S.W.; supervision, R.D.; project administration, R.D.; funding acquisition, R.D. and T.W. All authors have read and agreed to the published version of the manuscript.

Funding: This research was funded by the Key-Area Research and Development Program of Guangdong Province (Grant No. 2020B1111010002); National Natural Science Foundation of China (Grant No. 51679053; 12002404); Opening Fund for State Key Laboratory of Shipping Technology and Security; Guangdong Basic and Applied Basic Research Foundation (2019A1515110721), the China Postdoctoral Science Foundation (No. 2019M663243); the Fundamental Research Funds for the Central Universities (No.20lgpy52).

Data Availability Statement: Data is contained within the present article.

Conflicts of Interest: The authors declare no conflict of interest. The funders had no role in the design of the study; in the collection, analyses, or interpretation of data; in the writing of the manuscript, or in the decision to publish the results.

References

1. Lindstad, H.; Jullumstro, E.; Sandaas, I. Reductions in cost and greenhouse gas emissions with new bulk ship designs enabled by the Panama Canal expansion. *Energy Policy* **2013**, *59*, 341–349. [\[CrossRef\]](#)
2. Lindstad, H. Assessment of Bulk Designs Enabled by the Panama Canal Expansion. *Trans. Soc. Nav. Arch. Mar. Eng.* **2015**, *121*, 590–610.
3. Lindstad, H.E.; Rehn, C.F.; Eskeland, G.S. Sulphur Abatement Globally in Maritime Shipping. *Transp. Res. Part D* **2017**, *57*, 303–313. [\[CrossRef\]](#)
4. Lindstad, E.; Bø, T.I. Potential power setups, fuels and hull designs capable of satisfying future EEDI requirements. *Transp. Res. Part D* **2018**, *63*, 276–290. [\[CrossRef\]](#)
5. Sariöz, E. An optimization approach for fairing of ship hull forms. *Ocean Eng.* **2006**, *33*, 2105–2118. [\[CrossRef\]](#)
6. Hong, Z.C.; Zong, Z.; Li, H.T.; Hefazi, H.; Sahoo, P.K. Self-blending method for hull form modification and optimization. *Ocean Eng.* **2017**, *146*, 59–69. [\[CrossRef\]](#)
7. Rotteveel, E.; Hekkenberg, R.; Auke, V.D.P. Inland ship stern optimization in shallow water. *Ocean Eng.* **2017**, *141*, 555–569. [\[CrossRef\]](#)
8. Cerka, J.; Mickeviciene, R.; Ašmontas, Ž.; Norkevičius, L.; Žapnickas, T.; Djačkov, V.; Zhou, P. Optimization of the research vessel hull form by using numerical simulation. *Ocean Eng.* **2017**, *139*, 33–38. [\[CrossRef\]](#)
9. Deng, R.; Huang, D.B.; Yu, L.; Cheng, X.K.; Liang, H.G. Research on factors of a flow field affecting catamaran resistance calculation. *J. Harbin Eng. Univ.* **2011**, *32*, 141–147.
10. Cheng, X.D.; Feng, B.W.; Liu, Z.Y.; Chang, H.C. Hull surface modification for ship resistance performance optimization based on Delaunay triangulation. *Ocean Eng.* **2018**, *153*, 333–344. [\[CrossRef\]](#)
11. Hou, Y.H. Hull form uncertainty optimization design for minimum EEOI with influence of different speed perturbation types. *Ocean Eng.* **2017**, *140*, 66–72. [\[CrossRef\]](#)
12. Zheng, Q.; Chang, H.C.; Feng, B.W.; Liu, Z.Y.; Zhan, C.S. Research on knowledge-extraction technology in optimization of ship-resistance performance. *Ocean Eng.* **2019**, *179*, 325–336.
13. Kim, H.; Chi, Y. A new surface modification approach for CFD-based hull form optimization. *J. Hydrodyn. Ser. B* **2010**, *22*, 520–525. [\[CrossRef\]](#)
14. Feng, Y.K.; Chen, Z.G.; Dai, Y.; Wang, F.; Cai, J.Q.; Shen, Z.X. Multidisciplinary optimization of an offshore aquaculture vessel hull form based on the support vector regression surrogate model. *Ocean Eng.* **2018**, *166*, 145–158. [\[CrossRef\]](#)
15. Lin, Y.; Yang, Q.; Guan, G. Automatic design optimization of SWATH applying CFD and RSM model. *Ocean Eng.* **2019**, *172*, 146–154. [\[CrossRef\]](#)
16. Seok, W.; Kim, G.H.; Seo, J.; Rhee, S.H. Application of the design of experiments and computational fluid dynamics to bow design improvement. *J. Mar. Sci. Eng.* **2019**, *7*, 226. [\[CrossRef\]](#)
17. Priftis, A.; Boulougouris, E.; Turan, O.; Atzamos, A. Multi-objective robust early stage ship design optimization under uncertainty utilising surrogate models. *Ocean Eng.* **2020**, *197*, 106850. [\[CrossRef\]](#)
18. Papanikolaou, A.; Xing-Kaeding, Y.; Strobel, J.; Kanellopoulou, A.; Zaraphonitis, G.; Tolo, E. Numerical and Experimental Optimization Study on a Fast, Zero Emission Catamaran. *J. Mar. Sci. Eng.* **2020**, *8*, 657. [\[CrossRef\]](#)
19. Jeong, K.L.; Jeong, S.M. A Mesh Deformation Method for CFD-Based Hull form Optimization. *J. Mar. Sci. Eng.* **2020**, *8*, 473. [\[CrossRef\]](#)
20. Zhang, H.; Liu, Z.Y.; Zhan, C.S.; Feng, B.W. A sensitivity analysis of a hull's local characteristic parameters on ship resistance performance. *J. Mar. Sci. Technol.* **2016**, *21*, 592–600. [\[CrossRef\]](#)
21. Pechenyuk, A.V. Optimization of a hull form for decrease ship resistance to movement. *Comput. Res. Model.* **2017**, *9*, 57–65. [\[CrossRef\]](#)
22. Lindstad, H.; Sandaas, I.; Steen, S. Assessment of profit, cost, and emissions for slender bulk vessel designs. *Transp. Res. Part D Transp. Environ.* **2014**, *29*, 32–39. [\[CrossRef\]](#)
23. Lindstad, H.E.; Sandaas, I. Emission and Fuel Reduction for Offshore Support Vessels through Hybrid Technology. *J. Ship Prod. Des.* **2016**, *32*, 195–205. [\[CrossRef\]](#)
24. Lindstad, E.; Alterskjær, S.A.; Sandaas, I.; Solheim, A.; Vigsnes, J.T. Open Hatch Carriers—Future Vessel Designs & Operations. In Proceedings of the Conference proceedings SNAME 2017, Houston, TX, USA, 24 October 2017.
25. Du, P.; Ouahsine, A.; Toan, K.T.; Sergent, P. Simulation of ship maneuvering in a confined waterway using a nonlinear model based on optimization techniques. *Ocean Eng.* **2017**, *142*, 194–203. [\[CrossRef\]](#)
26. Khanh, T.T.; Ouahsine, A.; Naceur, H.; Wassifi, K.E. Assessment of ship maneuverability by using a coupling between a nonlinear transient maneuvering model and mathematical programming techniques. *J. Hydrodyn.* **2013**, *25*, 788–804. [\[CrossRef\]](#)
27. Holtrop, J. A statistical analysis of performance test results. *Int. Shipbuild. Prog.* **1977**, *24*, 23–28. [\[CrossRef\]](#)
28. Holtrop, J. A statistical re-analysis of resistance and propulsion data. *Int. Shipbuild. Prog.* **1984**, *31*, 272–276.

29. Holtrop, J. A statistical resistance prediction method with a speed dependent form factor. In Proceedings of the Scientific and Methodological Seminar on Ship Hydrodynamics (SMSSH '88), Varna, Bulgaria, 1 October 1988.
30. Holtrop, J.; Mennen, G. A statistical power prediction method. *Int. Shipbuild. Prog.* **1978**, *25*, 253–256. [[CrossRef](#)]
31. Holtrop, J.; Mennen, G. An approximate power prediction method. *Int. Shipbuild. Prog.* **1982**, *29*, 166–170. [[CrossRef](#)]
32. Birk, L. *Fundamentals of Ship Hydrodynamics: Fluid Mechanics, Ship Resistance and Propulsion*; John Wiley & Sons: Hoboken, NJ, USA, 2019; pp. 611–627.
33. Deng, R. Optimization of ship principal dimensions based on empirical methods. In *House Report*; Harbin Engineering University: Harbin, China, 2017; pp. 29–30.
34. Bales, N.K.; Cumins, W.E. The Influence of Hull Form on seakeeping. *Trans. SNAME* **1970**, *78*, 00007480.
35. Bales, N.K. Optimizing the seakeeping performance of destroyer type hulls. In Proceedings of the 13th Symposium on Naval Hydrodynamics, Tokyo, Japan, 6–10 October 1980.
36. Nomoto, K.; Taguchi, K.; Honda, K.; Hirano, S. On the Steering Qualities of Ships. *J. Zosen Kiokai* **1956**, *99*, 75–82. [[CrossRef](#)]
37. Nomoto, K.; Taguchi, K. On Steering Qualities of Ships (2). *J. Zosen Kiokai* **1957**, *101*, 57–66. [[CrossRef](#)]
38. Zhang, X.K.; Li, Y.K. Prediction of Ship Maneuverability Indices. *Navig. China* **2009**, *32*, 96–101.
39. Li, Z.B.; Zhang, X.K.; Zhang, Y. Prediction of maneuver ability indices for ships using SPSS. *Mar. Technol.* **2007**, *32*, 2–5.
40. Hong, B.G.; Yu, Y. Ship's, Kand T indices statistics analysis. *J. Dalian Marit. Univ.* **2000**, *26*, 29–33.
41. Yao, J.; Ren, Y.Q.; Li, X. Statistical Analysis of Fishing Vessel's Maneuverability Indexes K and T. *Navig. China* **2003**, *54*, 31–33.
42. Guo, C.Y.; Wu, T.C.; Zhang, Q.; Lou, W.Z. Numerical simulation and experimental studies on aft hull local parameterized non-geosim deformation for correcting scale effects of nominal wake field. *Brodogradnja* **2017**, *68*, 77–96. [[CrossRef](#)]
43. Deng, R.; Huang, D.B.; Li, J.; Cheng, X.K.; Lei, Y. Discussion on flow field CFD factors influencing catamaran resistance calculation. *J. Mar. Sci. Appl.* **2010**, *9*, 187–191. [[CrossRef](#)]